JACS
JOURNAL OF THE AMERICAN CHEMICAL SOCIETY
Communication
pubs.acs.org/JACS

ZSM-5 Zeolite Single Crystals with *b*-Axis-Aligned Mesoporous Channels as an Efficient Catalyst for Conversion of Bulky Organic Molecules

Fujian Liu,[†,∥] Tom Willhammar,[‡] Liang Wang,[§] Longfeng Zhu,[§] Qi Sun,[†] Xiangju Meng,[†] Wilder Carrillo-Cabrera,[⊥] Xiaodong Zou,*[,‡] and Feng-Shou Xiao*[,†]

[†]Key Lab of Applied Chemistry of Zhejiang Province, Zhejiang University, Hangzhou 310007, China

[‡]Berzelii Centre, EXSELLENT on Porous Materials and Department of Materials and Environmental Chemistry, Stockholm University, Stockholm SE-10691, Sweden

[§]College of Chemistry, Jilin University, Changchun 130012, China

[⊥]Max-Planck-Institut für Chemische Physik fester Stoffe, Dresden DE-01187, Germany

[∥]Institute of Applied Chemistry, Shaoxing University, Shaoxing 312000, China

Supporting Information

ABSTRACT: The relatively small and sole micropores in zeolite catalysts strongly influence the mass transfer and catalytic conversion of bulky molecules. We report here aluminosilicate zeolite ZSM-5 single crystals with *b*-axis-aligned mesopores, synthesized using a designed cationic amphiphilic copolymer as a mesoscale template. This sample exhibits excellent hydrothermal stability. The orientation of the mesopores was confirmed by scanning and transmission electron microscopy. More importantly, the *b*-axis-aligned mesoporous ZSM-5 shows much higher catalytic activities for bulky substrate conversion than conventional ZSM-5 and ZSM-5 with randomly oriented mesopores. The combination of good hydrothermal stability with high activities is important for design of novel zeolite catalysts. The *b*-axis-aligned mesoporous ZSM-5 reported here shows great potential for industrial applications.

Aluminosilicate zeolites with intricate micropores and strong acidity have been widely used as heterogeneous catalysts in the petrochemical and fine chemical industries.[1,2] However, relatively small and sole micropores in zeolites strongly hinder the diffusion of reactants and products, and thus the catalytic conversion of bulky molecules.[2,3] Using zeolite nanocrystals may overcome the diffusion problem, but separation of zeolite nanocrystals from a reaction mixture is difficult.[4] Recently, great efforts have been put forth to introduce mesopores/mesoporosity in zeolites through templating strategies.[5−10] Notably, these mesopores are randomly oriented in zeolite crystals. Controlling mesopore orientation in zeolites still remains a challenge. When ordered mesostructured carbon of CMK-3 with small pores (3−6 nm) was used as a hard template, disordered mesopores were formed as a result of aggregation of nanosized ZSM-5 crystals.[11] However, when ordered mesostructured carbons with large pores (6−40 nm) or polyquaternary ammonium surfactants were used, ordered mesopores surrounded by zeolite nanocrystal aggregates were obtained.[12,13b] Using designed bifunctional surfactants, stable single-unit-cell nanosheets of zeolite MFI were successfully prepared.[3c,13a] These results suggest that the formation of mesoporous zeolites with controllable orientations may need templates that can form large micelles or micelle aggregates with small curvatures. Large micelles could be obtained using, for example, triblock polymer of P123 and copolymer of PS_{215}−PEO_{100} in strongly acidic aqueous solution. They were used to synthesize ordered mesoporous silicas and carbons with large mesopores.[14,15] However, these amphiphilic copolymers often do not have strong interactions with silica species in basic media that is normally required for zeolite synthesis.[14,15] Therefore, it is still difficult to use conventional amphiphilic copolymers as templates to obtain mesopores in zeolite crystals. Here we show that appropriately designed amphiphilic copolymers with high molecular weight can direct the formation of zeolite ZSM-5 single crystals with *b*-axis-aligned mesopores (ZSM-5-OM). The open mesopores in ZSM-5-OM are very helpful for conversion of bulky organic molecules.

We used copolymer polystyrene-*co*-4-polyvinylpyridine (MW ≈ 1.6×10^5, PSt-*co*-P4VP) which was treated with methyl iodide, forming a cationic polymer (C-PSt-*co*-P4VP). The positively charged C-PSt-*co*-P4VP strengthens its interaction with the negatively charged silica species in the synthesis of zeolites and is thus a favorable template for synthesizing zeolites with oriented mesopores.[1] The formation of the cationic copolymer C-PSt-*co*-P4VP is confirmed by ^{1}H (Figure S1), ^{13}C NMR (Figure S2), and IR (Figure S3) spectra.[16]

Generally, aluminosilicate ZSM-5 is synthesized from a small organic template of tetrapropylammonium hydroxide (TPAOH). In this work, we used both small molecules of TPAOH and large copolymers of C-PSt-*co*-P4VP as organic templates for synthesizing ZSM-5 zeolite with *b*-axis-aligned mesopores (denoted as ZSM-5-OM). ^{13}C NMR spectroscopy shows that C-PSt-*co*-P4VP was essentially intact during the crystallization of ZSM-5-OM samples (Figures S4 and S5).

Received: January 15, 2012
Published: March 1, 2012

   dx.doi.org/10.1021/ja300078q | *J. Am. Chem. Soc.* 2012, 134, 4557−4560

X-ray diffraction (XRD) of calcined ZSM-5-OM gives well-resolved peaks characteristic of ZSM-5 zeolite (Figures S5 and S6a).[17] Calcined ZSM-5-OM exhibits a type IV N_2 adsorption/desorption isotherm with a hysteresis loop at a relative pressure of $0.45 < P/P_0 < 0.90$, characteristic of mesoporous solids (Figure S6b). The corresponding Barrett–Joyner–Halenda (BJH) pore size distribution shows mesopores in the range of 6–60 nm, with two peaks at 13 and 55 nm, respectively (Figure S6b inset). These results indicate that the ZSM-5-OM sample contains mesopores.

Figure 1 shows scanning electron microscopy (SEM) images of a calcined ZSM-5-OM sample synthesized in the presence of C-PSt-*co*-P4VP template. The sample consists of uniformly sized particles (1–2 μm) with rough surfaces, as seen in the low-magnification images (Figures 1a and S7). The particles have a hexagonal prism shape with *b*-axis-aligned mesopores (Figure 1b,c). Both small pores (about 10 nm) and large pores (about 50 nm) can be observed on the surface of the particles, as shown in the high-magnification images (Figures 1d and S7b,c).

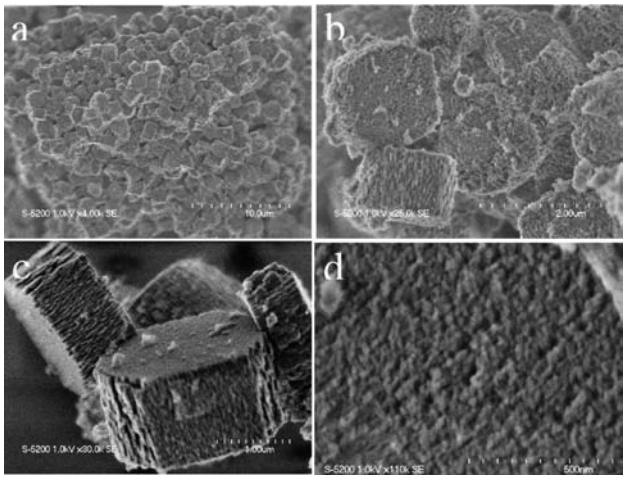

Figure 1. (a) Low- and (b–d) high-magnification SEM images of a calcined ZSM-5 sample synthesized in the presence of C-PSt-*co*-P4VP template showing oriented mesopores.

To further confirm the mesopores and the pore orientations, a calcined ZSM-5-OM sample was studied by transmission electron microscopy (TEM) (Figure 2). Electron diffraction shows that the entire particle is a single crystal, exhibiting a single diffraction pattern (Figure 2a). In order to reveal the inner pore structures of the crystals, focused ion beam (FIB) has been used to prepare thin slices perpendicular to each of the main crystallographic axes of ZSM-5-OM crystals (Figure S8). Images of the thin slices perpendicular to the *b*-axis show mesopores of 10–50 nm in size throughout the crystal (Figure 2b). The size range of the mesopores is in good agreement with the N_2 adsorption (6–60 nm). The mesopores are distributed within the crystal as well as near the surface of the crystal. High-resolution images taken along the *b*-axis show round mesopores (Figures 2c and S9a), which suggests that the pores run along the *b*-axis, perpendicular to the thin slice. The straight 10-ring microporous channels in ZSM-5 are well-ordered throughout the entire particle, which shows that the entire particle contains only one ZSM-5 single crystal, and not nanocrystal aggregates. HRTEM images taken along the *c*- and *a*-axis further confirm that the mesopores are running along the *b*-axis and the entire particle is a single crystal of ZSM-5. In addition, pores elongated along the *b*-axis or round were also observed along the *c*- and *a*-axis. This indicates that the mesopore channels have preferred orientations along the *b*-axis. The mesopore channels are not straight, and the width varies through the channels (Figures 2d,e and S9c). The difference in mesopore sizes might be related to the aggregation of the mesoscale amphiphilic copolymers.

Thermogravimetric analysis shows that ZSM-5-OM had a weight loss of 19.4% due to the removal of TPA^+ and C-PSt-*co*-

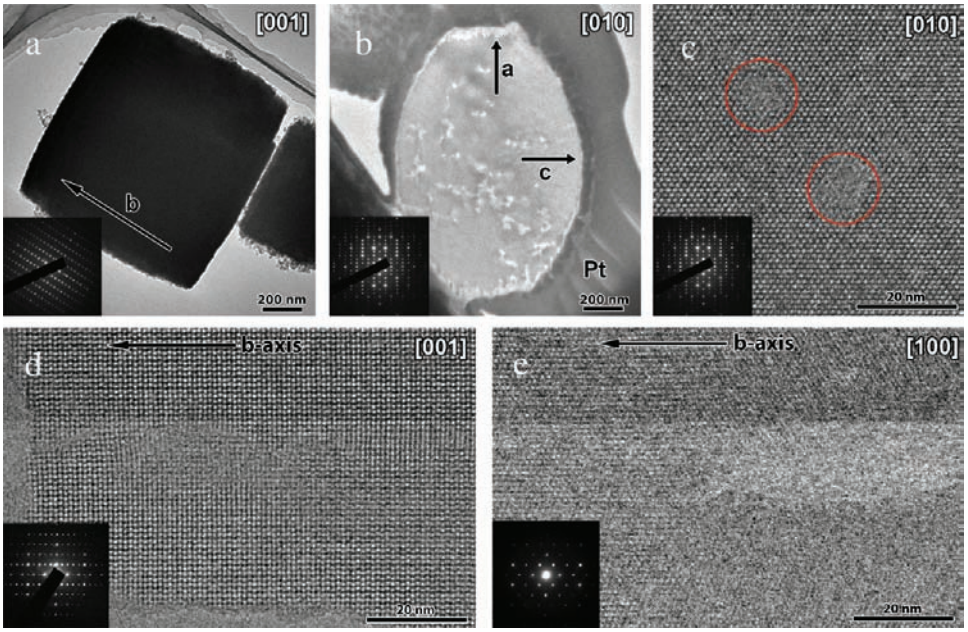

Figure 2. (a) TEM image of a ZSM-5-OM crystal taken along the *c*-axis. The corresponding electron diffraction pattern (inset) shows that the entire particle is a single crystal. (b) TEM image of a ZSM-5-OM crystal taken along the *b*-axis. (c–e) HRTEM images of thin slices of ZSM-5-OM viewed along the (c) *b*-, (d) *c*-, and (e) *a*-axis, with the crystals cut perpendicular to the *b*-, *c*-, and *a*-axis, respectively, by FIB. The *b*-axis is marked in (a), (d), and (e).

dx.doi.org/10.1021/ja300078q | *J. Am. Chem. Soc.* 2012, 134, 4557–4560

P4VP (Figure S10b). In contrast, conventional ZSM-5 exhibited a total weight loss of 11.3% (Figure S10a). Apparently, the larger weight loss in ZSM-5-OM is due to the presence of C-PSt-*co*-P4VP template that was removed during the heating in the sample. These results indicate that C-PSt-*co*-P4VP was occluded in the as-synthesized ZSM-5-OM. Subsequent removal of these templates led to the large pore volume and complex porosity in ZSM-5-OM, in agreement with the results obtained by nitrogen sorption (Figure S6b).

It is worth noting that the orientation of mesopores in ZSM-5-OM is along the *b*-axis as a result of the self-assembly of C-PSt-*co*-P4VP with ZSM-5 building units. This phenomenon might be related to the ZSM-5 structure (Figure S11). Among the three different faces [001], [010], and [101] of the ZSM-5 crystals, the [010] face is the most energetically favorable according to *ab initio* DFT calculations.[18] Possibly, the C-PSt-*co*-P4VP template prefers to occupy the [010] face in the self-assembly; therefore, *b*-axis-aligned mesopores could be formed in ZSM-5-OM. In addition, mesoporous channels in ZSM-5-OM match best with the *b*-axis of ZSM-5 crystals because the 10-ring microporous channels along the *b*-axis in ZSM-5 are straight, while the microporous channels along the *a*- and *c*-axis are zigzag. Recently, there have been many reports on mesoporous zeolites, but it is still a great challenge to control the orientation of the mesopores formed in zeolite single crystals.[5−10] In this work, by using a designed copolymer of C-PSt-*co*-P4VP, *b*-axis-aligned mesopores are successfully formed in single crystals of ZSM-5 zeolite.

Hydrothermal stability of porous materials is a crucial factor for their applications and has been intensively studied.[2,3] In the present study, the hydrothermal stability of *b*-axis-aligned mesoporous ZSM-5-OM was assessed by exposing to 100% steaming at 800 °C for 5 h. After this treatment, there was no obvious reduction of the crystallinity, surface area, and pore volume (Table 1, Figures S12 and S13), indicating the excellent hydrothermal stability of ZSM-5-OM.

Table 1. Textural Parameters of ZSM-5, Mesoporous ZSM-5-M, and *b*-Axis-Aligned Mesoporous ZSM-5-OM

sample[a]	S_{BET}, m^2/g	mesopore size,[b] nm	total pore volume,[c] cm^3/g	micropore volume, cm^3/g
ZSM-5	364	–	0.14	0.12
ZSM-5-M	390	17	0.30	0.09
ZSM-5-OM	365	13, 55	0.31	0.08
ZSM-5-OM[d]	370	18, 55	0.27	0.08

[a]ZSM-5 containing disordered mesopores was synthesized from using polydiallyldimethylammonium chloride, and ZSM-5-OM with *b*-axis-aligned mesopores was synthesized in the presence of C-PSt-*co*-P4VP template. Si/Al ratio was 37 in the starting gels and 37, 39, and 41 in the products of ZSM-5, ZSM-5-M, and ZSM-5-OM, respectively. [b]Calculated by BJH adsorption model. [c]Calculated by the relative pressure at 0.94. [d]100% steam treatment at 800 °C for 5 h.

Table 2 compares catalytic activities of the *b*-axis-aligned mesoporous ZSM-5-OM in conversion of bulky substrates to those of conventional ZSM-5 and ZSM-5 containing disordered mesopores (ZSM-5-M).[9a] In protection of benzaldehyde with pentaerythritol (PBP), ZSM-5 shows relatively low conversion at 12.8%. After introduction of disordered mesopores in the samples, ZSM-5-M exhibits higher activity at 49.5%. Interestingly, ZSM-5-OM gives very high activity at 88.4%, which is as good as that of ZSM-5 nanosheets (86%) under the same catalytic conditions.[3c]

Table 2. Catalytic Activities for Bulky Substrate Conversion over Various ZSM-5 Catalysts

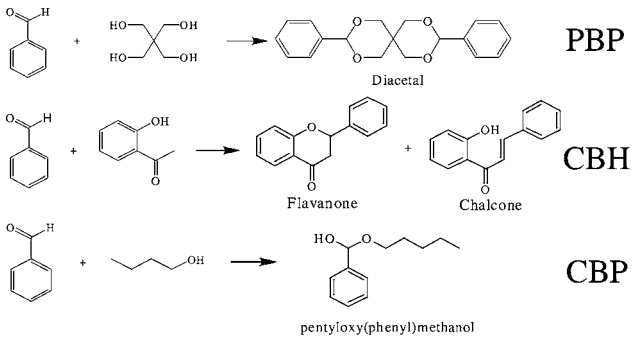

sample	catalytic conversion, % PBP[a]	CBH[b]	CBP[c]	note
ZSM-5	12.8	18.7	23.5	this work
ZSM-5-M	49.5	45.7	37.5	this work
ZSM-5-OM	88.4	90.8	46.8	this work
multilamellar ZSM-5 nanosheet[d]	86	48		ref 3c
unilamellar ZSM-5 nanosheet[e]	86	76		ref 3c

[a]Protection of benzaldehyde with pentaerythritol (PBP). [b]Condensation of benzaldehyde with hydroxyacetophenone (CBH). [c]Condensation of benzaldehyde with 1-pentanol (CBP). [d]Si/Al ratio 48. [e]Si/Al ratio 53.

In condensation of benzaldehyde with hydroxyacetophenone (CBH), ZSM-5 and ZSM-5-M give low (18.7%) and medium (45.7%) activities, respectively. In contrast, ZSM-5-OM is very active, giving a conversion of 90.8%. In condensation of benzaldehyde with 1-pentanol (CBP), ZSM-5, ZSM-5-M, and ZSM-5-OM have conversions at 23.5, 37.5, and 46.8%, respectively. Considering the similarities of ZSM-5, ZSM-5-M, and ZSM-5-OM in terms of Si/Al ratios, aluminum distribution, and acidic strength as well as a larger particle size of ZSM-5-OM than those of ZSM-5 and ZSM-5-M,[9a] the superior catalytic activities in conversion of bulky substrates over ZSM-5-OM compared to that over ZSM-5-M should be directly assigned to the contribution of *b*-axis-aligned mesopores in ZSM-5-OM. It is possible that almost all *b*-axis-aligned mesopores in zeolite crystals are opened to the surface of ZSM-5 crystals and are accessible by bulky molecules. In contrast, a majority of the disordered mesopores in the ZSM-5 crystals may be located in the interiors of the crystals and hardly accessible by the bulky molecules.

In summary, *b*-axis-aligned mesoporous ZSM-5 (ZSM-5-OM) has been successfully synthesized by using a designed amphiphilic copolymer (C-PSt-*co*-P4VP). This sample exhibited excellent hydrothermal stability and superior catalytic activities for conversion of bulky substrates. ZSM-5-OM shows great potential as an industrial catalyst, and its discovery provides new insights for future development of hydrothermally stable and active catalysts.

■ ASSOCIATED CONTENT

Supporting Information

Synthesis and characterization details. This material is available free of charge via the Internet at http://pubs.acs.org.

■ AUTHOR INFORMATION

Corresponding Author

fsxiao@zju.edu.cn; xzou@mmk.su.se.

Notes

The authors declare no competing financial interest.

■ ACKNOWLEDGMENTS

This work is supported by the State Basic Research Project of China (2009CB623507), National Natural Science Foundation of China (20973079 and U1162201), the Swedish Research Council (VR), the Swedish Governmental Agency for Innovation Systems (VINNOVA), Knut and Alice Wallenberg Foundation, and Göran Gustafsson Foundation.

■ REFERENCES

(1) (a) van Bekkum, H.; Flanigen, E. M.; Jacobs, P. A.; Jansen, J. C. *Introduction to Zeolite Science and Practice*; Elsevier: Amsterdam, 2001. (b) Breck, D. W. *Zeolite Molecular Sieves*; Krieger: Malabar, 1984.

(2) (a) Corma, A. *Chem. Rev.* **1997**, *97*, 2373. (b) Cundy, C. S.; Cox, P. A. *Chem. Rev.* **2003**, *103*, 663. (c) Corma, A. *Chem. Rev.* **1995**, *95*, 559.

(3) (a) Davis, M. E. *Nature* **2002**, *417*, 813. (b) Hartmann, M. *Angew. Chem., Int. Ed.* **2004**, *43*, 5880. (c) Choi, M.; Na, K.; Kim, J.; Sakamoto, Y.; Terasaki, O.; Ryoo, R. *Nature* **2009**, *461*, 246. (d) Jiang, J. X; Jorda, J. L.; Yu, J. H.; Baumes, L. A.; Mugnaioli, E.; Diaz-Cabanas, M. J.; Kolb, U.; Corma, A. *Science* **2011**, *333*, 1131. (e) Zou, X.; Conradsson, T.; Klingstedt, M.; Dadachov, M. S.; O'Keeffe, M. *Nature* **2005**, *437*, 716.

(4) (a) Tosheva, L.; Valtchev, V. *Chem. Mater.* **2005**, *17*, 2494. (b) Schoeman, B. J.; Sterte, J.; Otterstedt, J. E. *Zeolites* **1994**, *14*, 110.

(5) (a) Jacobsen, C. J. H.; Madsen, C.; Houzvicka, J.; Schmidt, I.; Carlsson, A. *J. Am. Chem. Soc.* **2000**, *122*, 7116. (b) Perez-Ramirez, J.; Christensen, C. H.; Egeblad, K.; Christensen, C. H.; Groen, J. C. *Chem. Soc. Rev.* **2008**, *37*, 2530.

(6) (a) Tao, Y.; Kanoh, H.; Kaneko, K. *J. Am. Chem. Soc.* **2003**, *125*, 6044. (b) Tao, Y.; Kanoh, H.; Abrams, L.; Kaneko, K. *Chem. Rev.* **2006**, *106*, 896.

(7) (a) Choi, M.; Cho, H. S.; Srivastava, R.; Venkatesan, C.; Choi, D.-H.; Ryoo, R. *Nat. Mater.* **2006**, *5*, 718. (b) Choi, M.; Srivastava, R.; Ryoo, R. *Chem. Commun.* **2006**, 4380. (c) Shetti, V. N.; Kim, J.; Sricastava, R.; Choi, M.; Ryoo, R. *J. Catal.* **2008**, *254*, 296.

(8) (a) Wang, H.; Pinnavaia, T. J. *Angew. Chem., Int. Ed.* **2006**, *45*, 7603. (b) Park, D. H.; Kim, S. S.; Wang, H.; Pinnavaia, T. J.; Papapetrou, M. C.; Lappas, A. A.; Triantafyllidis, K. S. *Angew. Chem., Int. Ed.* **2009**, *48*, 7645. (c) Chen, L. H.; Li, X. Y.; Tian, G.; Li, Y.; Rooke, J. C.; Zhu, G. S.; Qiu, S. L.; Yang, X. Y.; Su, B.-L. *Angew. Chem., Int. Ed.* **2011**, *50*, 11156.

(9) (a) Xiao, F.-S.; Wang, L. F.; Yin, C. Y.; Lin, K. F.; Di, Y.; Li, J.; Xu, R.; Su, D. S.; Schlogl, R.; Yokoi, T.; Tatsumi, T. *Angew. Chem., Int. Ed.* **2006**, *45*, 3090. (b) Meng, X. J.; Nawaz, F.; Xiao, F.-S. *Nano Today* **2009**, *4*, 292. (c) Fu, W.; Zhang, L.; Tang, T.; Ke, Q.; Wang, S.; Hu, J.; Fang, G.; Li, J.; Xiao, F.-S. *J. Am. Chem. Soc.* **2011**, *133*, 15346. (d) Tang, T. D.; Yin, C. Y.; Wang, L. F.; Ji, Y. Y.; Xiao, F.-S. *J. Catal.* **2008**, *257*, 125. (e) Wang, L. F.; Zhang, Z.; Yin, C. Y.; Shan, Z. C.; Xiao, F.-S. *Microporous Mesoporous Mater.* **2010**, *131*, 58.

(10) (a) Sun, Y.; Prins, R. *Angew. Chem., Int. Ed.* **2008**, *47*, 8478. (b) Zhou, J. A.; Hua, Z. L.; Cui, X. Z.; Ye, Z. Q.; Cui, F. M.; Shi, J. L. *Chem. Commun.* **2010**, *46*, 4994. (c) Moller, K.; Yilmaz, B.; Jacubinas, R. M.; Muller, U.; Bein, T. *J. Am. Chem. Soc.* **2011**, *133*, 5284. (d) Gu, F. N.; Wei, F.; Yang, J. Y.; Lin, N.; Lin, W. G.; Lin, Y.; Zhu, J. H. *Chem. Mater.* **2010**, *22*, 2422.

(11) Yang, Z. X.; Xia, Y. D.; Mokaya, R. *Adv. Mater.* **2004**, *16*, 727.

(12) (a) Fan, W.; Snyder, M. A.; Kumar, S.; Lee, P. S.; Yoo, W. C.; McCormick, A. V.; Penn, R. L.; Stein, A.; Tsapatsis, M. *Nat. Mater.* **2008**, *7*, 984. (b) Lee, P.-S.; Zhang, X. Y.; Stoeger, J. A.; Malek, A.; Fan, W.; Kumar, S.; Yoo, W. C.; Hashimi, S. A.; Penn, R. L.; Stein, A.; Tsapatsis, M. *J. Am. Chem. Soc.* **2011**, *133*, 493. (c) Cho, H. S.; Ryoo, R. *Microporous Mesoporous Mater.* **2012**, *151*, 107. (d) Chen, H. Y.; Wydra, J.; Zhang, X. Y.; Lee, P. S.; Wang, Z. P.; Fan, W.; Tsapatsis. *J. Am. Chem. Soc.* **2011**, *133*, 12390.

(13) (a) Na, K.; Choi, M.; Park, W.; Sakamoto, Y.; Tarasaki, O.; Ryoo, R. *J. Am. Chem. Soc.* **2010**, *132*, 4169. (b) Na, K.; Jo, C.; Kim, J.; Cho, K.; Jung, J.; Seo, Y.; Messinger, R. J.; Chmelka, B. F.; Ryoo, R. *Science* **2011**, *333*, 328.

(14) Zhao, D.; Feng, J.; Huo, Q.; Melosh, N.; Fredrickson, G. H.; Chmelka, B. F.; Stucky, G. D. *Science* **1998**, *279*, 548.

(15) Deng, Y. H.; Yu, T.; Wan, Y.; Shi, Y. F.; Meng, Y.; Gu, D.; Zhang, L. J.; Huang, Y.; Liu, C.; Wu, X. J.; Zhao, D. *J. Am. Chem. Soc.* **2007**, *129*, 1690.

(16) (a) Chen, D. Y.; Peng, H. S.; Jiang, M. *Maromolecules* **2003**, *36*, 2576. (b) Zhang, B. Q.; Chen, G. D.; Pan, C. Y.; Luan, B.; Hong, C. Y. *J. Appl. Polym. Sci.* **2006**, *102*, 1950. (c) Krishnan, S.; Ward, R. J.; Hexemer, A.; Sohn, K. E.; Lee, K. L.; Angert, E. R.; Fischer, D. A.; Kramer, E. J.; Ober, C. K. *Langmuir* **2006**, *22*, 11255.

(17) Baerlocher, Ch.; McCusker, L. B.; Olson, D. H. *Atlas of Zeolite Framework Types*, 6th ed.; Elsevier: Amsterdam, 2007.

(18) Shan, Z. C.; Wang, H.; Meng, X. J.; Liu, S.; Wang, L.; Wang, C. Y.; Li, F.; Lewis, J. P.; Xiao, F.-S. *Chem. Commun.* **2011**, *47*, 2048.